

Neutron star structure in a Quark Model with Excluded Volume Correction *

R. M. Aguirre and A. L. De Paoli.

Departamento de Física, Fac. de Ciencias Exactas,
Universidad Nacional de La Plata.
C. C. 67 (1900) La Plata, Argentina.

February 25, 2019

Abstract

We study the effects of the finite size of baryons on the equation of state of homogeneous hadronic matter. The finite extension of hadrons is introduced in order to improve the performance of field theoretical models at very high densities. We simulate the in-medium averaged baryon-baryon strong repulsion at very short distances by introducing a Van der Waals like normalization of the baryon fields. This is done in the framework of the Quark Meson Coupling model, that allows to take care of the quark structure of baryons. Since within this model the confinement volume evolves with the fields configuration, the treatment is not equivalent to a simple hard-core potential. We investigate the phase transition to quark matter and the structure of neutron stars. We have found significant corrections at high densities.

PACS : 12.39.Ba, 13.75.Ev, 21.30.Fe, 21.65.+f, 26.60.+c

*This work was partially supported by the CONICET, Argentina.

1 Introduction

Investigation of hadronic matter at extreme conditions of density and temperature is a current issue of research, since the study of its properties will eventually shed some light over the recovering of QCD symmetries [1, 2]. The phase diagram of hadronic matter is expected to be very complex, exhibiting exotic phases like superfluidity, meson condensates, dibaryon condensate, etc. The gradual emergence of quark droplets would finally lead to a transition to deconfined quark matter. Everyone of these phenomena affects the equation of state and could have macroscopic manifestations as, for example, in the structure of stars.

In most hadronic matter studies point-like particles are assumed. However, taking care of the spatial extension of baryons was recognized as an essential point in the study of the collective phenomena at very high densities [3]. Instead, at densities below the nuclear matter saturation density, the finite volume effects are expected to be small.

It is worthy to mention that there are only a few field theoretical models which consistently include the baryon spatial extension, the most commonly used are the Skyrme and bag-like models. In the first case the inclusion of finite baryon density effects is not straightforward due to the topological character of its solutions [4]. On the other hand further refinements of the original MIT bag model allow to deal with medium effects upon the hadron structure [5, 6, 7]. Within this scheme there were recent efforts to include the repulsion between overlapping bags, through effective short-ranged quark-quark correlations [7].

The authors attempted previously to take into account finite volume correction using a Van der Waals-like method to study nuclear matter with lambda hyperons [8]. The total volume appearing in the thermodynamical quantities was replaced by the available volume, in accordance with related investigations [9, 10, 11, 12, 13].

In the present work we want to generalize this approach to study the properties of hadronic matter including the octet of low lying baryons, and to check out their influence over the transition to quark matter. The resulting equation of state is applied to study the composition of neutron stars. In accordance with our previous study [8] we introduce these corrections at the level of the normalization of the baryon fields in the hadronic sector of the Quark Meson Coupling (QMC) model [5, 6]. The motivation for such a procedure is to parameterize in compact form the strong baryon-baryon repulsion at very short distances. We focus our attention on the high density regime, therefore we do not care about the details of the interactions but only about their statistical average.

In the QMC model the size of the confining volume has its own dynamical evolution, therefore the approach is not directly related to the "hard-core" potentials of nuclear physics.

In the next section we give a resume of the QMC model. In section 3 we describe neutron star matter and the phase transition to quark matter. Numerical results and discussion are given in section 4, conclusions are drawn in section 5.

2 The Quark Meson Coupling Model

The QMC model [5, 6] may be viewed as an extension of the Quantum Hadro-Dynamics (QHD) models [14, 15]. Relativistic Hadron Field Theories have provided a good description of nuclear matter near the saturation density, and of the finite nuclei also. For this purpose only a small number of free parameters is required. Mean field approximation is suited for the aim of these theories, since the treatment of matter at medium and high densities do not require the detailed structure of the interactions.

In the QMC model baryons are represented as non-overlapping spherical bags containing three valence quarks; the bag radius changes dynamically with the medium density. Baryons interact by the exchange of σ , ω and ρ mesons coupled directly to the confined quarks. It has been found that these extra degrees of freedom, provided by the internal structure of the baryon, lead to quite acceptable values of the nuclear matter compressibility at saturation. Despite the explicit quark fields in the QMC model, hadronic thermodynamical properties are evaluated in such a way that baryons are handled as point-like particles with an effective mass M_B^* which depends on the σ field.

To describe briefly the QMC model, one considers baryons as spherical MIT bags where quarks are confined. The Dirac equation for a quark of flavor q , ($q = u, d, s$), of current mass m_q and I_3^q third isospin component, in the mean field approximation is given by

$$(i\gamma^\mu \partial_\mu - g_\omega^q \gamma^0 \omega_0 - g_\rho^q I_3^q \gamma^0 b_0 - m_q^*) \Psi^q = 0. \quad (2.1)$$

In this equation all meson fields have been replaced by their mean field values. Mesons couple linearly only to non-strange quarks, i.e. $g_\sigma^s = g_\omega^s = g_\rho^s = 0$. Therefore the parameters m_q^* are given by

$$\begin{aligned} m_{u,d}^* &= m_{u,d} - g_\sigma^{u,d} \sigma, \\ m_s^* &= m_s. \end{aligned} \quad (2.2)$$

For a spherically symmetric bag of radius R_b representing a baryon of class b , the normalized quark wave function $\Psi_b^q(r, t)$ is given by

$$\Psi_b^q(r, t) = \mathcal{N}_b^{-1/2} \frac{e^{-i\varepsilon_{qb} t}}{\sqrt{4\pi}} \begin{pmatrix} j_0(x_{qb} r/R_b) \\ i\beta_{qb} \vec{\sigma} \cdot \hat{r} j_1(x_{qb} r/R_b) \end{pmatrix} \chi^q, \quad (2.3)$$

where χ^q is the quark spinor and

$$\varepsilon_{qb} = \frac{\Omega_{qb}}{R_b} + g_\omega^q \omega_0 + g_\rho^q I_3^q b_0, \quad (2.4)$$

$$\mathcal{N}_b = R_b^3 [2\Omega_{qb}(\Omega_{qb} - 1) + R_b m_q^*] \frac{j_0^2(x_{qb})}{x_{qb}^2}, \quad (2.5)$$

$$\beta_{qb} = \left[\frac{\Omega_{qb} - R_b m_q^*}{\Omega_{qb} + R_b m_q^*} \right]^{1/2}, \quad (2.6)$$

with $\Omega_{qb} = [x_{qb}^2 + (R_b m_q^*)^2]^{1/2}$. The eigenvalue x_{qb} is solution of the equation

$$j_0(x_{qb}) = \beta_q j_1(x_{qb}), \quad (2.7)$$

which arises from the boundary condition at the bag surface.

In this model the ground state bag energy is identified with the baryon mass M_b^* ,

$$M_b^* = \frac{\sum_q n_q^b \Omega_{qb} - z_{0b}}{R_b} + \frac{4}{3} \pi B R_b^3, \quad (2.8)$$

where n_q^b is the number of quarks of flavor q inside the bag. The bag constant B represents the difference of energy per unit volume between the vacuum with and without broken QCD symmetry, it is numerically adjusted to get definite values for the proton bag radius. The zero-point motion parameters z_{0b} are fixed to reproduce the baryon spectrum at zero density.

Eq. (2.8) shows that the baryon effective mass is a function of the bag radius R_b . In the original MIT bag calculations R_b is a constant fixed at zero baryon density, but in the QMC it is a variable dynamically adjusted to reach the equilibrium of the bag in the dense hadronic medium. We use the equilibrium condition proposed in ref. [8]

$$-\frac{n_s^b}{n^b} \left(\frac{\partial M_b^*}{\partial v_b} \right)_{\sigma, x_{qb}} = \frac{1}{3\pi^2} \sum_{b'} \int_0^{k_{b'}} \frac{dk k^4}{\sqrt{M_{b'}^*{}^2 + k^2}}, \quad (2.9)$$

obtained by minimizing the energy density ϵ with respect to the effective bag volume v_b , keeping constant the total volume V [9, 10]. It must be noted that Eq. (2.9) differs from the standard QMC condition [6], i.e.

$$\left(\frac{\partial M_b^*}{\partial R_b} \right)_{\sigma} = 0, \quad (2.10)$$

both prescriptions coincide only in the case of vanishing density.

Once M_b^* has been defined microscopically, the hadronic thermodynamics in the QMC model resembles that of the Quantum Hadrodynamics. In the mean field approximation for homogeneous infinite static matter all meson fields are replaced by their averaged values, i. e.

$$\sigma = \sigma_0 = -\frac{1}{m_{\sigma}^2} \sum_b \frac{dM_b^*}{d\sigma} n_s^b, \quad (2.11)$$

$$\omega_{\mu} = \omega_0 \delta_{\mu 0} = \frac{1}{m_{\omega}^2} \sum_B g_{\omega}^b n^b \delta_{\mu 0}, \quad (2.12)$$

$$b_{\mu}^a = b_0 \delta_{\mu 0} \delta_{a3} = \frac{1}{m_{\rho}^2} \sum_b g_{\rho}^b I_3^b n^b \delta_{\mu 0} \delta_{a3}, \quad (2.13)$$

where $a = 1, 2, 3$ runs over all isospin directions and I_3^b is the third isospin component of baryon b . In our calculations we used the values $m_{\sigma} = 550 MeV$, $m_{\omega} = 783 MeV$, and $m_{\rho} = 770 MeV$ for the meson masses.

The dispersion relation for the b-baryon is

$$k_0^b = \sqrt{M_b^{*2} + \vec{k}^2} \pm g_\omega^b \omega_0 \pm g_\rho^b I_3^b b_0, \quad (2.14)$$

for particle (+) and antiparticle (−) solutions. Within the MFA at zero temperature only the particle solutions contribute.

The scalar (n_s^b) and baryonic (n^b) densities are defined with respect to the ground state of the hadronic matter $|GS\rangle$ composed of baryons filling the Fermi sea up to the state with momentum k_b

$$n_s^b = \langle GS | \bar{\Psi}^b \Psi^b | GS \rangle = \vartheta \frac{1}{\pi^2} M_b^* \int_0^{k_b} dk \frac{k^2}{\sqrt{M_b^{*2} + k^2}}, \quad (2.15)$$

$$n^b = \langle GS | \Psi^{\dagger b} \Psi^b | GS \rangle = \vartheta \frac{k_b^3}{3\pi^2}. \quad (2.16)$$

In Eqs. (2.15) and (2.16) the factor ϑ is included for future use and it takes on the value $\vartheta = 1$ for point-like baryons.

In the next section we describe hadronic matter in β -equilibrium and electrically neutral, therefore we also consider leptons treated as free Dirac particles. The leptonic density n_l is related to the Fermi momentum k_l by means of

$$n^l = \langle GS | \Psi^{\dagger l} \Psi^l | GS \rangle = \frac{k_l^3}{3\pi^2}. \quad (2.17)$$

Given a distribution of baryonic species we can calculate the total energy density ϵ_H and pressure P_0 of hadronic matter for point-like baryons

$$\begin{aligned} \epsilon_H &= \frac{1}{2} m_\sigma^2 \sigma_0^2 + \frac{1}{2} m_\omega^2 \omega_0^2 + \frac{1}{2} m_\rho^2 b_0^2 \\ &+ \frac{\vartheta}{\pi^2} \sum_b \int_0^{k_b} dk k^2 \sqrt{M_b^{*2} + k^2} \\ &+ \frac{1}{\pi^2} \sum_l \int_0^{k_l} dk k^2 \sqrt{m_l^2 + k^2}, \end{aligned} \quad (2.18)$$

$$P_0 = \sum_b \mu_0^b n^b + \sum_l \mu^l n^l - \epsilon_H, \quad (2.19)$$

where $\mu_0^b = k_0^b(k_b)$ (see Eq. (2.14)) and μ^l are the chemical potentials for point-like baryons and leptons, respectively.

At high densities, the strong repulsive component of the baryon-baryon interaction appears as a consequence of the internal structure of the particles. This short ranged repulsion can be assimilated to a simplified model where baryons are described as extended objects over a spherical volume of radius R , where R reflects the range of the repulsion. Therefore the fraction of available space is reduced as compared to the case of point-like particles. A similar approach has been applied to study the phase transition of nuclear matter to the quark-gluon plasma [9, 10] and in heavy-ion collisions [11, 12].

Finite size baryons are assumed as non-overlapping, so their motion is restricted to the available space V' defined as [9, 10]

$$V' = V - \sum_b N^b v_b, \quad (2.20)$$

with N^b the total number of baryons of class b inside the volume V , and v_b is the effective volume per baryon of this class. Hence if we renormalize the particle (antiparticle) wave function replacing V' for V , the effective baryon fields Ψ can be written as

$$\begin{aligned} \Psi^b(x) = (V')^{-1/2} \sum_{\vec{k}, s} & [a^b(\vec{k}, s) u^b(\vec{k}, s) e^{-ik^\mu x_\mu} \\ & + b^{\dagger b}(\vec{k}, s) v^b(\vec{k}, s) e^{ik^\mu x_\mu}] \end{aligned} \quad (2.21)$$

in terms of the Fock space operators a and b , for particle and antiparticle respectively. In this way the finite size of the baryons is automatically accounted for into the field dynamics.

It is interesting to note that for a mixture of different baryons the excluded volume is not exactly the same for all the species [16]. To simplify the discussions, in this paper we neglect these small differences.

The effective volume per baryon v_b is proportional to the actual baryon volume, i.e. for spherical volumes of radius R_b

$$v_b = \alpha \frac{4\pi}{3} R_b^3, \quad (2.22)$$

and for sharp rigid spheres α is a real number ranging from 4, in the low density limit, to $3\sqrt{2}/\pi$, which corresponds to the maximum density allowed for non overlapping spheres, in a face centered cubic arrange. Since we wish to study the high density regime of homogeneous isotropic matter, we shall adopt $\alpha = 3\sqrt{2}/\pi$ in all our calculations. Thus $v_b = 4\sqrt{2}R_b^3$ and the upper limit for the baryon density is given by $1/v_{max} = \sqrt{2}/(8R_{max}^3)$, where R_{max} denotes the biggest radius among all present baryonic classes.

In order to see how volume corrections appear in our approach, we shall use the renormalized field of Eq. (2.21) to calculate the relationship between baryon densities n^b and the Fermi momenta k_b

$$n^b = V^{-1} \int_V dx^3 \langle GS | \Psi^{\dagger b} \Psi^b | GS \rangle = (1 - \sum_{b'} n^{b'} v_{b'}) \frac{k_b^3}{3\pi^2}, \quad (2.23)$$

where $\sum_{\vec{k}} \rightarrow V'/(2\pi^3) \int dk^3$ has been used.

This result is equivalent to Eq. (2.16) if the factor ϑ takes on the value

$$\vartheta = 1 - \sum_b n^b v_b, \quad (2.24)$$

for finite baryon effective volumes v_b . In the limit $v_b \rightarrow 0$ one recovers the point-like expressions.

Eq. (2.23) shows that short-ranged correlations couple non linearly the baryons among themselves, in a density dependent way.

We can solve explicitly Eq. (2.23) for n_b as a function of all the Fermi momenta k_b , namely

$$n^b = \frac{1}{(1 + \sum_{b'} \frac{k_{b'}^3}{3\pi^2} v_{b'})} \frac{k_b^3}{3\pi^2}. \quad (2.25)$$

Since ϑ in our approach depends explicitly upon the baryonic densities, the chemical potentials get an extra term, i.e.

$$\mu^b = \left(\frac{\partial \epsilon_H}{\partial n_b} \right)_{\substack{n_{b'} \\ b' \neq b}} = \mu_0^b + \Delta\mu^b, \quad (2.26)$$

$$\Delta\mu^b = \frac{v_b}{3\pi^2} \sum_{b'} \int_0^{k_{b'}} \frac{dk k^4}{\sqrt{M_{b'}^{*2} + k^2}}. \quad (2.27)$$

The energy density ϵ_H is given by Eq.(2.18) with ϑ defined as in Eq.(2.24). The total pressure acquires an additional term ΔP as compared to the pressure of point-like baryons P_0 Eq. (2.19)

$$P_H = P_0 + \Delta P = P_0 + \sum_b n^b \Delta\mu^b. \quad (2.28)$$

In our approach only the baryonic states receive an explicit correction due to short range forces, through the normalization of the fields Ψ^b . It must be stressed that the meson mean field values are completely determined from the baryonic sources, that already include finite size corrections in ϑ . Leptons do not experiment strong interactions, and in this sense they are taken as point-like particles.

To resume, in our approach matter properties are determined applying the set of equations (2.11) to (2.18), together with (2.26)-(2.28) for a fixed value of the total baryon density n , using the value of ϑ given in (2.24). The limit of validity of the assumptions corresponds to densities such that the center of mass of baryons are at a distance greater than $2R$ apart. Otherwise the simple quasiparticle picture breaks down.

3 Quark matter phase transition and the structure of neutron stars

Neutron star matter is electrically neutral and it has reached equilibrium against β -decay. Neutrinos completely escaped after the characteristic time

has elapsed. The relative abundance of the different baryonic species are determined by these conditions. In the present work we consider the nucleon duplet (n,p), the Λ -hyperon, the Σ triplet, the Ξ duplet, and two lepton species, electron and muon.

In the chemical equilibrium the following relationships are fulfilled for the baryonic and leptonic chemical potentials

$$\mu^b = \mu^n + Q_b \mu^e \quad (\text{if } b \text{ baryon is present}), \quad (3.1)$$

$$\mu^e = \mu^\mu \quad (\text{if muons are present}), \quad (3.2)$$

with Q_b the electric charge relative to the electron one for the class b of baryons, μ^b given by Eq. (2.26) and $\mu^l = k_0^l(k_l) = \sqrt{m_l^2 + k_l^2}$.

Mean field equations are solved for fixed total baryon density n and zero total electric density charge

$$n = \sum_b n^b, \quad (3.3)$$

$$0 = \sum_b Q^b n^b - \sum_l n^l, \quad (3.4)$$

where the first sum runs over the eight baryonic species and the second one over the two lepton species.

Having more than one conserved charge, we adopt the treatment of [17] to describe phase transitions, therefore a smooth crossover between hadron and quark matter must be expected.

The Eqs. (2.11)-(2.13) determine the meson fields $(\sigma_0, \omega_0, b_0)$ when Eq. (2.8) has been solved, and together with Eqs. (2.16), (3.1)-(3.4) provide the baryon and lepton densities (n^b, n^l) , all the Fermi momenta (k_b, k_l) and chemical potentials (μ^b, μ^l) .

If for a given density the phase transition to quark matter is reached then the previous set of equations must be modified. It is expected a mixed phase coexistence region where charge neutrality and β -equilibrium are preserved, but there is no reason for their conservation in each phase separately. Instead baryon charge conservation and electric neutrality are required for both phases together [17]

$$n = (1 - \chi) n_H + \chi n_Q, \quad (3.5)$$

$$0 = (1 - \chi) \sum_b Q^b n^b + \chi \sum_q Q^q n^q - \sum_l n^l,$$

where $n_H = \sum_b n^b$, $n_Q = \sum_q n^q/3$ are respectively the hadron and quark contribution to the baryon number density; $n^q = N_c k_q^3/(3\pi^2)$ is the number density of quarks for N_c colors, k_q is the Fermi momentum, and Q^q is the

electric charge relative to the electron charge for the flavor q . The quantity χ is the volume fraction corresponding to the quark matter phase. The β -equilibrium condition for quarks reads: $\mu_d = \mu_s = \mu_u + \mu_e$, with $\mu_q = \sqrt{m_q^2 + k_q^2}$. In the mixed phase the last relation must be supplemented with $\mu_n = 3\mu_d - \mu_e$ and the mechanical equilibrium condition $P_H = P_Q$, where $P_{H,Q}$ are the pressures in each phase. It must be noted that the case $\chi = 0(1)$ in Eq. (3.5) comprises the pure hadron (quark) matter phase instance.

The energy density in the mixed phase can be similarly expressed as $\epsilon = (1 - \chi)\epsilon_H + \chi\epsilon_Q$. The thermodynamical quantities for the quarks are evaluated by introducing the non-perturbative effects represented by the bag constant B in the energy density of free quarks plus leptons

$$\begin{aligned}\epsilon_Q &= B + \frac{N_c}{\pi^2} \sum_q \int_0^{k_q} dk k^2 \sqrt{m_q^2 + k^2} \\ &\quad + \frac{1}{\pi^2} \sum_l \int_0^{k_l} dk k^2 \sqrt{m_l^2 + k^2},\end{aligned}\quad (3.6)$$

$$P_Q = \sum_q \mu_q n^q + \sum_l \mu_l n^l - \epsilon_Q. \quad (3.7)$$

The equation of state emerging from this calculation can be used to evaluate the properties of neutron stars. The stellar radius R and mass M are obtained by solving the Tolman-Oppenheimer-Volkoff relativistic equations for a spherically symmetric (non-rotating) neutron star

$$\begin{aligned}\frac{dP}{dr} &= -(G/c^2) \frac{[\epsilon(r) + P(r)][m(r) + 4\pi r^3 P(r)/c^2]}{r^2[1 - 2(G/c^2)m(r)/r]}, \\ m(r) &= \int_0^r 4\pi r'^2 [\epsilon(r')/c^2] dr'.\end{aligned}\quad (3.8)$$

Starting from a given value ϵ_c for the central energy density, these equations are integrated outward until a radius $R(\epsilon_c)$ is reached for which the pressure P is zero, and $M = m(R)$ is defined.

To determine more accurately the radius of the star, we use the equation of state given in reference [18] for baryon densities below $0.1n_0$.

The moment of inertia I for a slowly rotating star can be obtained through [18, 19]

$$I = \frac{8\pi}{3} \int_0^R r^4 e^{-\nu(r)/2} \frac{[\epsilon(r) + P(r)]/c^2}{\sqrt{1 - 2(G/c^2)m(r)/r}} \frac{\bar{\omega}(r)}{\Omega} dr, \quad (3.9)$$

where Ω is the uniform angular velocity of the star as seen by a distant inertial observer, $\Omega \ll (c/R) \sqrt{(G/c^2)M/R}$. The radial function $\nu(r)$ is solution of the differential equation

$$\frac{d\nu}{dr} = 2(G/c^2) \frac{[m(r) + 4\pi r^3 P(r)/c^2]}{r^2[1 - 2(G/c^2)m(r)/r]}, \quad (3.10)$$

with the boundary condition $\nu(R) = -\ln[1 - 2(G/c^2)M/R]$. The relative angular velocity $\bar{\omega}(r)$ measured with respect to the local dragged inertial frame, is the solution of

$$\frac{d}{dr} \left[r^4 j(r) \frac{d\bar{\omega}(r)}{dr} \right] + 4r^3 \bar{\omega}(r) \frac{dj}{dr} = 0, \quad (3.11)$$

with $j(r) = \sqrt{1 - 2(G/c^2)m(r)/r} \exp[-\nu(r)/2]$ inside the star. Since $j(r) = 1$ for $r \geq R$, $\bar{\omega}(r)$ has the form $\bar{\omega}(r) = \Omega[1 - 2(G/c^2)I/r^3]$ outside.

A useful quantity in astronomical observations is the surface redshift z given by

$$z = [1 - 2(G/c^2)M/R]^{-1/2} - 1. \quad (3.12)$$

Numerical values obtained in our approach can be found in Table 2.

4 Numerical Results

Within the present model the quark masses take on its current values $m_u = m_d = 5\text{MeV}$, $m_s = 150\text{MeV}$. The parameter B represents a universal constant and therefore is the same for all the baryon bags. We avoid any speculation about its density dependence. We consider the range $170\text{MeV} \leq B^{1/4} \leq 210\text{MeV}$ that yields a proton bag radius within the range $0.6\text{fm} \leq R_p \leq 0.8\text{fm}$ (see Table 1). For a given value of B the set of parameters z_{0b} are adjusted to obtain the experimental baryon masses at zero density.

Since mesons interact directly with quarks, the corresponding meson-baryon couplings are related to the quark-meson couplings g_ϕ^q ($\phi = \sigma, \omega, \rho$, $q = u, d$) in a simple way [6]. Denoting as g_ϕ^b the coupling of the ϕ -meson to b -baryon,

$$\begin{aligned} g_\sigma^b &= N_{ns}^b g_\sigma^u, \\ g_\omega^b &= N_{ns}^b g_\omega^u, \\ g_\rho^b &= g_\rho^u, \end{aligned} \quad (4.0.13)$$

where N_{ns}^b is the non-strange quark content of baryon b . Thus, once g_σ^u, g_ω^u and g_ρ^u are known, the full set of baryon-meson couplings is determined. To fix their numerical values we require the symmetric nuclear matter properties at saturation, i.e. baryon density, binding energy and symmetry energy, to be reproduced

$$\begin{aligned} n_0 &= 0.15\text{fm}^{-3}, \\ E_b &= (\epsilon/n)_0 - Mc^2 = -16\text{MeV}, \\ a_s &= \frac{1}{2} \left(\frac{\partial^2(\epsilon/n)}{\partial t^2} \right)_{t=0} = 35\text{MeV}, \end{aligned} \quad (4.0.14)$$

where $t = (n_n - n_p)/n$ and $M = 938.92\text{MeV}/c^2$ is the averaged free nucleon rest mass.

As expected, the coupling values are sensitive to the inclusion or not of the excluded volume corrections. Both instances are considered in Table 1.

For practical considerations, we have chosen the values $B^{1/4} = 169.93, 187.83$ and 210.85 MeV that will be denoted respectively as (a), (b) and (c) in the following. They yield a proton bag radius $R_p = 0.8, 0.7$ and 0.6 fm respectively. In addition the inclusion (CC) or not (NC) of the excluded volume correction have been considered.

In all cases we start in the hadronic phase increasing the baryonic density until the coexistence conditions are satisfied. This occurs at critical densities n_{cl} which are shown in Table 1. The numerical value of n_{cl} increases with B , and it does not appear at all for the case (c)-NC, at least within the range of validity of the non-overlapping bags assumption. The lowest value obtained $n_{cl} \simeq n_0$ corresponds to $B^{1/4} = 169.93 \text{ MeV}$, is not able for a true physical consideration and it is retained only for illustrative purposes.

For all the bag constant values considered here, the non-overlapping bag hypotheses breaks down in the NC approach, before the pure quark plasma has taken place. Thus pure stars with a quark content can not be described within this frame. In the CC instance the upper density threshold n_{cu} for the mixed phase is enlarged as B increases, for $n > n_{cu}$ only pure quark matter can be found.

It must be noted that the same B is used consistently in the QMC and free quark descriptions.

In Fig. 1 we show the meson mean field values in the hadronic and mixed phases. Differences between the NC and CC treatments become appreciable for $n > n_0$. As can be seen, the ρ meson amplitude has a sudden change of slope at the phase transition due to the change in the isospin composition of the hadronic sector in the neighborhood of n_{cl}

In the same figure the excluded volume correction factor ϑ is displayed as a function of the baryon density, ϑ seems to become almost constant at sufficiently high densities.

The proton bag radius R_p and its effective mass M_p^* can be examined in Fig. 2. A faster radius decrease is observed in the CC instance. In this last case a dropping of about $15\% - 20\%$ in R_p is obtained before the hadronic matter has completely disappeared, this strong compression of the baryonic bags helps the deconfinement mechanism. The effective mass M_p^* exhibits a monotonous decrease as a function of the baryonic density, the rate of variation at low densities is attenuated by both decreasing B and/or including volume corrections.

The composition of star matter is depicted in Fig. 3 for cases (b) and (c). The onset of the quark phase in the NC instance suppress the hyperons that could be present if it would not have take place. Otherwise in the CC approach new hyperon species appear even in the mixed phase. It must be noted a noticeable diminution of the relative lepton abundance in the mixed phase.

The equation of state for (b) and (c) are represented in Fig. 4. The energy density ϵ in the mixed phase varies in the range $0.3 - 1.1 \text{ GeV fm}^{-3}$ for (b)-CC, whereas it ranges between $0.6 - 2.0 \text{ GeV fm}^{-3}$ for the set (c)-CC. In the CC treatment the pressure shows sudden changes of slope at the extreme points of the mixed phase, which are absent in the NC case.

The results for neutron star structure based on these equations of state

are displayed in Fig. 5. They are given in units of the solar mass $M_\odot = 1.9889 \cdot 10^{30} kg$.

The masses \overline{M} , radii \overline{R} and moments of inertia \overline{I} for the maximum star masses are recorded in Table 2. We have found that $1.51 \leq \overline{M}/M_\odot \leq 1.88$, a result which is above the experimental lower limit $M/M_\odot = 1.44$ accepted for binary pulsars. In all the cases we have obtained $12 km \lesssim \overline{R} \lesssim 13 km$, being \overline{R} rather insensitive to the internal structure, at least for these particular examples.

The Fig. 5 also shows that the maxima are reached in a plateau, and they are enhanced in the CC cases. In addition, the composition of the star depends on the selected value of the bag parameter B . For example, taking the CC results, the (b)-CC choice predicts that a mixed phase of deconfined quarks and hadrons can be found in a central core with radius of about $7.48 km$, which contains 45% of \overline{M} and contributes 18% to the moment of inertia \overline{I} of the star. Meanwhile in the (c)-CC case the hadron-quark mixed phase extends up to $4.31 km$ and it encloses only 12% of \overline{M} ; its contribution to the moment of inertia \overline{I} is small, around 1.5%. We can also mention that the option (a)-CC, although not physically reliable, predicts a star structure which includes a pure quark core, surrounded by a crust of mixed phase and an outer shell of hadrons. The maximum star mass allowed in this case is $1.42 M_\odot$ with a radius of $9.28 km$.

5 Conclusions

We have studied high density matter in a treatment that links coherently the nonperturbative QCD effects (represented by the bag constant B) for both confined and deconfined quarks, although in a schematic way. The in-medium averaged short range interaction among baryons is represented by the excluded volume correction factor ϑ . This correction becomes effective at medium/high densities contributing to the onset of a deconfined quark phase. It is also the cause of sudden changes in the compressibility at the extreme points of the hadron-quark mixed phase. As a common feature of the starting point of this coexistence region we have found an abrupt change in the rate of growth of the vector iso-vector meson as well as in the lepton concentration relative to the baryon density.

The effects on the neutron star structure has been examined, we found that the maximum star mass is enhanced by both growing B and introducing excluded volume corrections. The CC approach leads also to a small increase of the star radius at the maximum mass, as compared to the respective NC case.

The CC treatment enlarges the range of applicability of the QMC model, allowing to reach the pure quark matter phase. In our approach this transition takes place at baryon densities where excluded volume corrections are significative, and they should be included if one wishes to describe properly the structure of massive systems like neutron stars.

References

- [1] H. Hatsuda and T. Kunihiro, Phys. Rep. **247**, 221 (1994).
- [2] G. E. Brown and M. Rho, Phys. Rep. **269**, 333 (1996).
- [3] J. Kapusta, Phys. Rev. D **23**, 2444 (1981).
- [4] A. Rakhimov, M. M. Musakhanov, F. C. Khanna and U. Yakhshiev, Phys. Rev. C **58**, 1738 (1998).
- [5] P. A. M. Guichon, Phys. Lett. **B200**, 235 (1988).
- [6] K. Saito and A. W. Thomas, Phys. Lett. **B327**, 9 (1994); Phys. Rev. C **51**, 2757 (1995);
K. Tsushima, K. Saito and A. W. Thomas, Phys. Lett. **B411**, 9 (1997);
K. Tsushima, K. Saito, J. Haidenbauer and A. W. Thomas, Nucl. Phys. **A630**, 691 (1998).
- [7] K. Saito, K. Tsushima and A. W. Thomas, LANL Report *nucl-th/9901084*.
- [8] R. Aguirre and A.L. De Paoli, LANL Report *nucl-th/9907087*.
- [9] S. Kagiyama, A. Nakamura, T. Omodaka, Z. Phys. C **53**, 163 (1992);
56, 557 (1992).
- [10] S. Kagiyama, A. Minaka, A. Nakamura, Prog. Theor. Phys. **89**, 1227 (1993).
- [11] D. H. Rischke, M. I. Gorenstein, H. Stöcker and W. Greiner, Z. Phys. C **51**, 485 (1991).
- [12] J. Cleymans and H. Satz, Z. Phys. C **57**, 135 (1993);
J. Cleymans , M. I. Gorenstein, J. Stålnacke, E. Suhonen, Phys. Scripta **48**, 277 (1993);
H. Kouno, K. Koide, T. Mitsumori, N. Noda, A. Hasegawa, M. Nakano, Prog. Theor. Phys. **96**, 191 (1996);
G. D. Yen, M. I. Gorenstein, W. Greiner, S. N. Yang, Phys. Rev. C **56**, 2210 (1997);
M. I. Gorenstein, H. Stöcker, G. D. Yen, S. N. Yang, W. Greiner, J. Phys. G **24**, 1777 (1998).
- [13] C. P. Singh, B. K. Patra, K. K. Singh, Phys. Lett. **B387**, 680 (1996).
- [14] J. D. Walecka, Ann. Phys. **83**, 491 (1974); Phys. Lett. **B59**, 109 (1975).
- [15] B. D. Serot and J. D. Walecka, Advan. Nucl. Phys. **16**, 1 (1986); Int. J. Mod. Phys. E **6**, 515 (1997).
- [16] M. I. Gorenstein, A. P. Kostyuk and Ya. D. Krivenko, J. Phys G **25**, L75 (1999).

- [17] N. K. Glendenning, Phys. Rev. D **46**, 1274 (1992).
- [18] G. Baym, C. Pethick and P. Sutherland, Astrophys. J. **170**, 299 (1971).
- [19] J. B. Hartle, Astrophys. J. **150**, 1005 (1967);
A. Akmal, V. R. Pandharipande and D. G. Ravenhall, Phys. Rev. C **58**, 1804 (1998).

$B^{1/4}[MeV]$	$R_p[fm]$	Case	$g_\sigma^{u,d}$	$g_\omega^{u,d}$	$g_\rho^{u,d}$	n_{cl}/n_0	n_{cu}/n_0
169.93	0.8	NC	5.747	2.756	8.668	1.20	—
		CC	4.678	1.701	7.600	1.06	3.98
187.83	0.7	NC	5.858	2.872	8.582	2.10	—
		CC	5.311	2.372	7.948	1.87	6.58
210.85	0.6	NC	5.993	3.007	8.523	—	—
		CC	5.702	2.747	8.151	3.91	10.17

Table 1: The quark-meson couplings $g_{\sigma,\omega,\rho}^{u,d}$ for each of the three values of the bag constant B used in our calculations, and for each of the approaches with excluded volume correction (CC) and without it (NC). The last two columns show the lower (n_{cl}) and upper (n_{cu}) densities of the mixed hadron-quark phase.

$B^{1/4}[MeV]$	Case	\bar{M}/M_\odot	$\bar{R}[km]$	$n_{c\max}/n_0$	\bar{z}	$\bar{I}[10^{30}kg\ km^2]$
187.83	NC	1.506	11.70	6.886	0.2701	137.8
	CC	1.592	13.02	5.148	0.2513	184.1
210.85	NC	1.672	12.38	5.800	0.2897	181.5
	CC	1.879	12.69	5.507	0.3330	227.1

Table 2: Neutron star properties for each of the chosen bag constants used in our calculations and for each of the approaches: with excluded volume correction (CC) and without it (NC). The star mass \bar{M} relative to the sun mass, the star radius \bar{R} , the central baryon density ($n_{c\max}$), the surface redshift \bar{z} and the moment of inertia \bar{I} (for a slowly rotating star), all corresponding to the star with maximum mass.

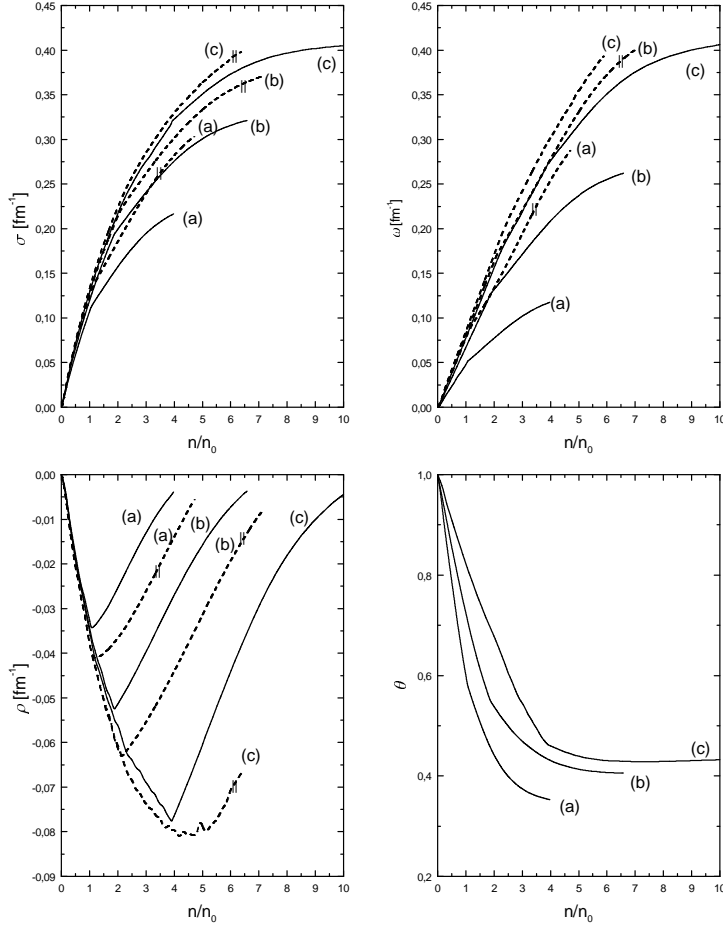


Figure 1: Meson mean field values σ , ω and b_0 as functions of the baryon density relative to the saturation nuclear density n_0 . The results with (without) excluded volume correction are represented with solid (dashed) lines. The different bag constant values $B^{1/4} = 169.9, 187.8$, and 210.8 MeV are distinguished with the labels a , b and c respectively. In the right lower corner the volume correction factor ϑ is displayed in terms of the baryon density. The CC curves are plotted up to the upper density threshold n_{cu} . Numerical values for the density threshold n_{cl} and n_{cu} can be seen in Table 1. The double bars crossing the NC curves indicate the limit of validity of the approach due to the breakdown of the non-overlapping bags hypotheses.

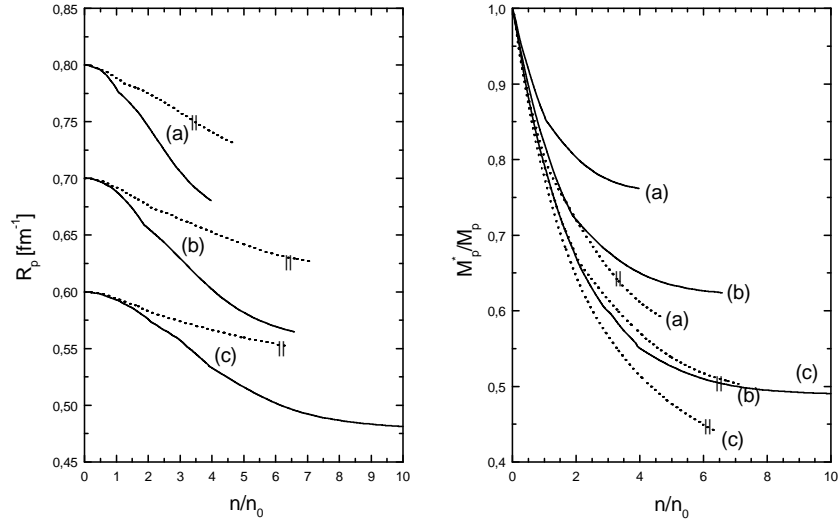


Figure 2: The in-medium proton bag radius R_p and proton mass M_p^* relative to its vacuum values. The line and label convention are the same as in Fig. 1.

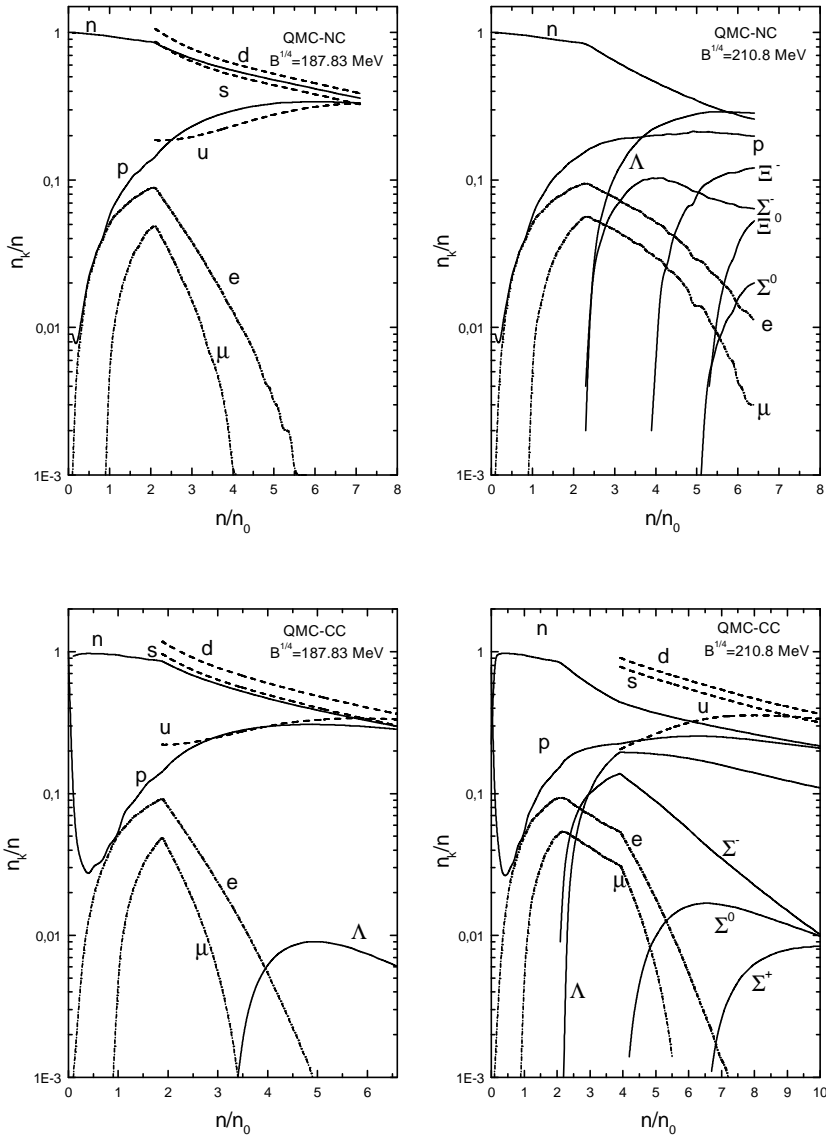


Figure 3: The baryon and quark composition of the star matter in terms of the baryon density for the bag constant values $B^{1/4} = 187.8$ and 210.85 MeV, for the NC and CC cases. The line convention is explained in each panel.

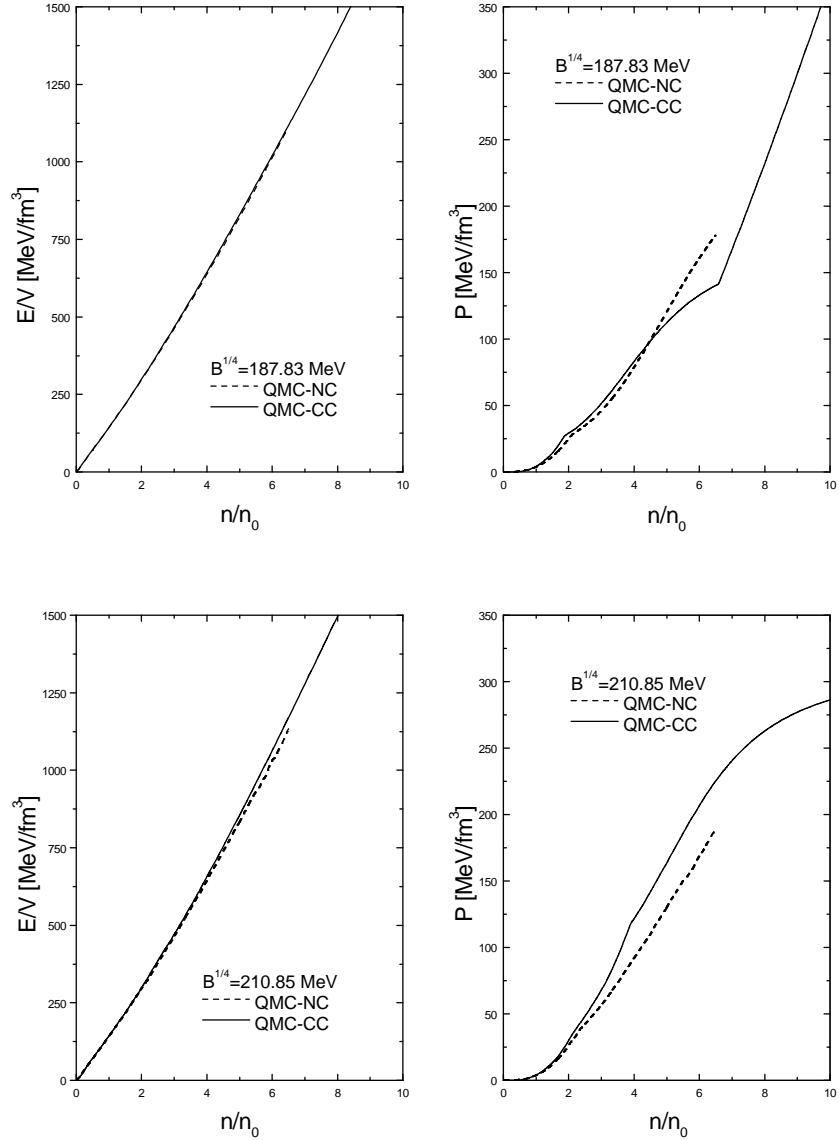


Figure 4: The total energy density ϵ and the pressure P for star matter in terms of the baryon density for the bag constant values $B^{1/4} = 187.8$ and 210.85 MeV, for the NC and CC cases. For the last instance the pressure varies continuously, but it has discontinuous derivatives at n_{cl} and n_{cu} (see Table 1).

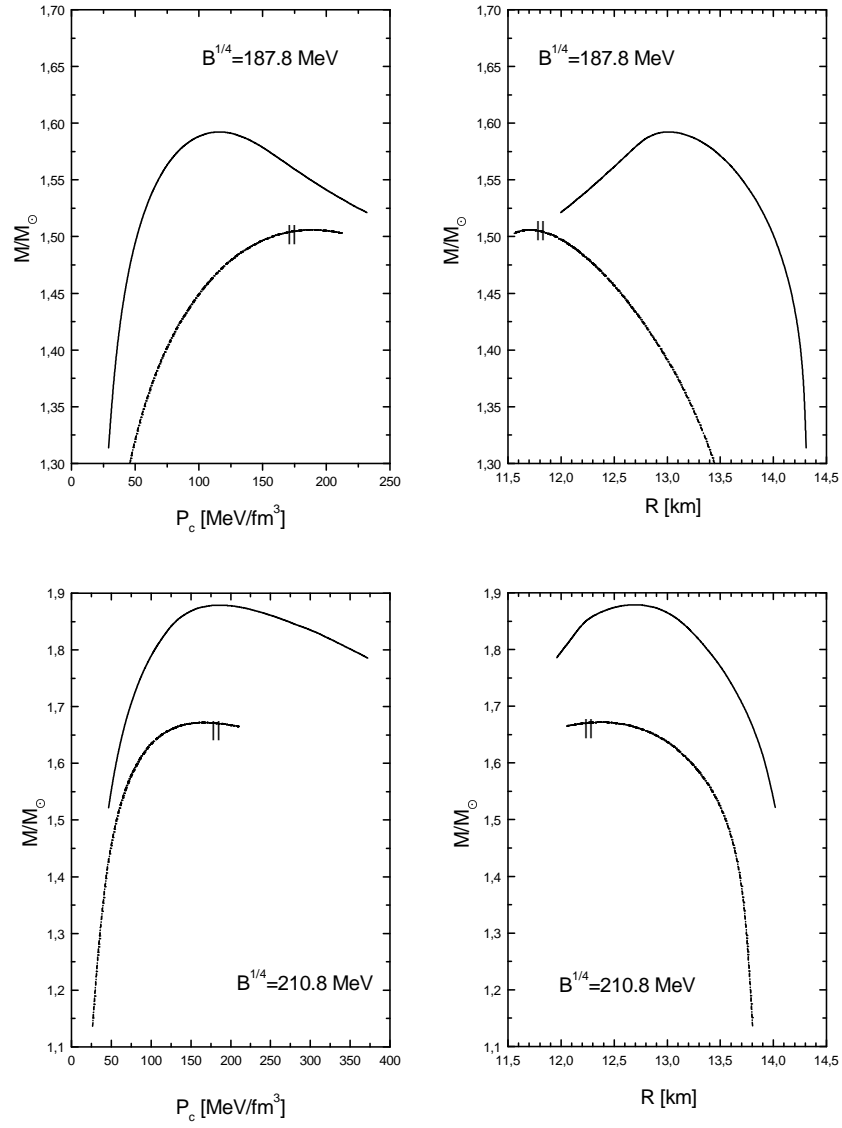


Figure 5: The relative gravitational star mass M/M_\odot in terms of the central pressure P_c (left panel) and M/M_\odot in terms of the star radius R (right panel). Excluded volume corrections enhance both \bar{M} and \bar{R} . Numerical values can be examined in Table 2.